

Duplex treatment on AISI D2 tool steel: plasma nitriding and reactive deposition of TiN and TiAlN films via magnetron sputtering

Marcio Luiz Moretti¹ , Abel André Cândido Recco¹ 

¹Universidade do Estado de Santa Catarina, Departamento de Física. Rua Paulo Malschitzki, 200, Campus Universitário Prof. Avelino Marcante, 89219-710, Joinville, SC, Brasil.

e-mail: marcio.lui.moretti@hotmail.com.br, abel.recco@udesc.br

ABSTRACT

In this work, titanium nitride (TiN) and titanium aluminum nitride (TiAlN) films have been obtained via triode magnetron sputtering. The films were deposited using a direct current source on plasma nitrided AISI D2 tool steel (duplex treatment), non-nitrided steel, and silicon. The nitrided layer was characterized by scanning electron microscopy (SEM), Vickers microhardness, and X-ray diffraction (XRD). The films were characterized by SEM and XRD. The mechanical properties of the coatings were determined using the instrumented indentation technique (IIT) and the adhesion of the film to the substrate was qualitatively evaluated using the Rockwell C test. Both films presented no significant variation in hardness (H) and elastic modulus (E). However, compared to the films obtained in non-nitrided steel, the duplex treatment improved the film-substrate adhesion. The improvement in adhesion can be attributed to the preliminary plasma nitriding treatment and the compressive loads acting on the nitrided surface.

Keywords: AISI D2 steel; duplex treatment; plasma nitriding; reactive deposition; triode magnetron sputtering.

1. INTRODUCTION

The AISI type D tool steels are usually used in metallic materials such as dies, thread rolling, punches, and chucks for cold working [1]. During the forming process, the friction between the steel and the material to be plastically deformed raises the working pressure and generates stress concentration. As a result, the surface of tool steels overheats, and their wear rate increases [2].

A technology used to increase the useful life of these products is the surface hardening of the steel using treatments such as quenching, electrodeposition, plasma treatment, ion implantation, thermal spraying, chemical vapor deposition, and physical vapor deposition [3].

Among the treatments mentioned, physical vapor deposition using compounds based on nitrides such as TiN, $Ti_{(1-x)}Al_xN$, CrN, and $Ti_{(1-x)}C_xN$ allows the obtaining of films with high hardness, high wear resistance, and low friction coefficient without modifying the properties in the substrate core [4].

Another technique used to increase the wear resistance of tool steel is duplex treatment. This method combines two surface treatments, plasma nitriding and thin film deposition via magnetron sputtering [5]. The compressive loads acting on the nitrided layer provide mechanical support to the substrate surface [6], increasing the load loading and unloading capacity, which may improve the film-substrate adhesion quality [7–9].

TiN and TiAlN films were obtained on plasma-treated and untreated steel in this work. Plasma nitriding was performed in a working atmosphere containing nitrogen, hydrogen, and argon gases. The depositions were carried out on the surface of untreated and plasma treated steel (duplex treatment). Both depositions were carried out in the reactive mode using a mixture of argon and nitrogen gases.

Therefore, this study has aimed to evaluate the influence of the duplex treatment on the intrinsic and functional properties of TiN and $Ti_{0.41}Al_{0.59}N$ films that were obtained via triode magnetron sputtering on AISI D2 tool steel.

2. MATERIALS AND METHODS

2.1. Raw materials

As substrates, AISI D2 tool steel cylinders for cold working and silicon plates (100) were used. The steel has a diameter of 15.9 mm and a thickness of 9.8 mm. The silicon has a rectangular shape of approximately $20.0 \pm 2.0 \text{ mm} \times 15.0 \pm 2.0 \text{ mm} \times 0.6 \pm 0.1 \text{ mm}$ thick.

Table 1 shows the chemical composition of the steel substrate in weight percentage, measured by optical emission spectroscopy, in a Shimadzu equipment model OES-5500 II.

Using steel, it was possible to qualitatively evaluate the adhesion of the films to the substrates, determine the crystalline structure, and measure the mechanical properties of the nitrided layer and the films. Silicon plates were used to determine the average thickness and microstructure of the films [10].

Ti (99.99% purity) and $\text{Ti}_{0.5}\text{Al}_{0.5}$ (99.50% purity) by weight were used as targets. Both targets consist of metallic cylinders with a diameter of 100 mm and a thickness of 6 mm.

2.2. Surface treatments

Figure 1 shows a schematic of surface treatments performed on AISI D2 steel.

This work used plasma nitriding and reactive deposition treatments in different reactors, which characterizes the discontinuous duplex treatment.

Initially, the residues present on the surface of the substrates were removed through the following procedures: the steel surface was sanded using silicon carbide sandpaper with a granulometry of 100, 240, 320, 400, 600, and 1200 MESH and polished using an abrasive based on alumina particles (Al_2O_3) with $1.0 \mu\text{m}$ granulometry. Then, the steel samples were submerged in isopropyl alcohol in an ultrasonic cleaner for 10 minutes. The silicon samples were cleaned with liquid detergent submerged in running water and washed with isopropyl alcohol in an ultrasonic cleaner for 10 minutes.

Table 1: Chemical composition of AISI D2 steel, in weight percentage.

| ELEMENT | CHEMICAL COMPOSITION (wt. %) |
|-----------------|------------------------------|
| Carbon (C) | 1.4 ± 0.1 |
| Silicon (Si) | 0.3 ± 0.1 |
| Manganese (Mn) | 0.3 ± 0.1 |
| Nickel (Ni) | 0.1 ± 0.1 |
| Chromium (Cr) | 13.3 ± 0.1 |
| Molybdenum (Mo) | 0.8 ± 0.1 |
| Cobalt (Co) | 0.1 ± 0.1 |
| Tungsten (W) | 0.2 ± 0.1 |
| Vanadium (V) | 0.9 ± 0.1 |
| Iron (Fe) | Balance |

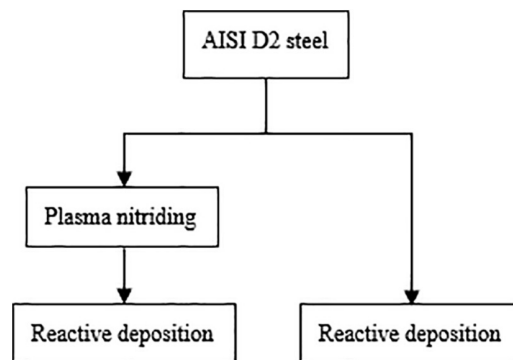


Figure 1: Schematic surface treatment performed on AISI D2 steel.

Plasma nitriding was performed in a working atmosphere containing 5% nitrogen (N_2), 74% hydrogen (H_2), and 21% argon (Ar) by volume for 120.0 ± 0.5 minutes. Temperature, current, and voltage were kept constant and equal to 500 ± 5 °C, 240 ± 2 mA, and 762 ± 2 V, respectively [10].

The reactive depositions of the TiN and $Ti_{0.41}Al_{0.59}N$ films were performed using a magnetron system composed of a stainless steel grid [11] and a voltage source in direct current. During the depositions, flow rates of 4.6 ± 0.1 sccm of N_2 in the TiN films and 6.8 ± 0.2 sccm of N_2 in the $Ti_{0.41}Al_{0.59}N$ films were used. Between the substrate and the TiN film, an intermediate layer of titanium (Ti) was deposited. The metallic Ti layer was obtained using an Ar flow rate of 2.8 ± 0.1 sccm, the pressure of 0.4 ± 0.1 Pa, and a current of 2.0 ± 0.2 A for 2.0 ± 0.5 minutes [10].

The target plasma cleaning was performed on all depositions using an Ar flow rate of 2.8 ± 0.1 sccm at 2.0 ± 0.2 A direct current for 2.0 ± 0.5 minutes.

The process parameters used in the film depositions are shown in Table 2.

Temperature, pressure, current density, and Ar flow were kept constant at 300 ± 5 °C, 0.9 ± 0.1 Pa, 2.0 ± 0.5 A, and 2.8 ± 0.1 sccm, respectively [10].

2.3. Characterizations

Table 3 correlates the substrates used, the type of treatment, and the characterization techniques performed. The steel nitrided layer was characterized by X-ray diffraction (XRD), Vickers microhardness profile, and scanning electron microscopy (SEM). The coatings were characterized by XRD, Rockwell C, instrumented indentation technique (IIT), and SEM.

To measure the microhardness of the nitrided layer of the steel, a Shimadzu HMV-2T microhardness tester was used, consisting of a diamond indenter with a pyramidal base. The first indentation was performed on the top of the surface of the nitrided layer with a load of 980.7 mN, which was applied for 10 seconds. A total of fifteen measurements were performed. Then, a load of 245.2 mN was applied for 10 seconds at 10 μ m and 20 μ m below the surface of the nitrided layer. The subsequent measurements were performed every 10 μ m up to 180 μ m concerning the top of the surface of the nitrided layer. In these indentations, the applied load and test execution time were constant and equal to 980.7 mN and 10 seconds, respectively. For each load application point, five measurements were performed. The measured values were analyzed using the Easy Test software.

The X-ray diffraction patterns were obtained using the Shimadzu XRD-600 model diffractometer. The diffractograms were collected from the nitrided surface of the steel and the deposited films on nitrided steel (duplex treatment). Copper K- α 1 radiation with a wavelength of 1.5406 Å, a voltage of 40 keV, a current of 30.0 mA, and a scanning speed of 2.0° per minute were used. The crystalline phases were identified through the diffracted lines (2θ) and the respective interplanar distances, which were analyzed using the OriginPro software adjustment and compared with the Inorganic Crystal Structure Database (ICSD).

To analyze the microstructure of the nitrided layer of the steel and the coatings deposited on the silicon, a scanning electron microscope with the field emission gun Jeol JSM-670 1F was used. To reveal the microstructure of the nitrided layer of the steel, the substrate was sectioned on an Isomet 4000 cutting machine with a diamond disc. Then the

Table 2: Films deposition process parameters.

| FILM | TREATMENT | N_2 FLOW (sccm) | TIME (min) | V BIAS (V) |
|-----------------------|--|-------------------|----------------|-------------|
| TiN | Reactive deposition | 4.6 ± 0.1 | 54.0 ± 0.5 | -30 ± 2 |
| TiN | Duplex: plasma nitriding and reactive deposition | 4.6 ± 0.1 | 54.0 ± 0.5 | -30 ± 2 |
| $Ti_{0.41}Al_{0.59}N$ | Reactive deposition | 6.8 ± 0.2 | 60.0 ± 0.5 | -50 ± 2 |
| $Ti_{0.41}Al_{0.59}N$ | Duplex: plasma nitriding and reactive deposition | 6.8 ± 0.2 | 60.0 ± 0.5 | -50 ± 2 |

Table 3: Substrates and characterization techniques.

| SUBSTRATE | TREATMENT | CHARACTERIZATION TECHNIQUES |
|-----------|---------------------|-------------------------------------|
| Silicon | Reactive deposition | SEM |
| AISI D2 | Plasma nitriding | XRD, Vickers microhardness, EDS-SEM |
| AISI D2 | Reactive deposition | XRD, Rockwell-C, IIT |

two sections were glued together with the nitrated surfaces laid out against each other. To analyze the microstructure and determine the average thickness of the films, the silicon substrates were fractured to reveal the cross-section. The images generated via SEM were processed using the ImageJ software. Nine measurements were performed per coating.

The coating's hardness (H) and elastic modulus (E) were determined using the CETR-Apex indenter coupled to the atomic force microscope. The tip used was a Berkovich diamond, and the indenter tip penetrated a maximum of 10% of the total thickness of the coatings. The value considered for Poisson's ratio (ν) in the TiN films was 0.19 [12] and in the $Ti_{0.41}Al_{0.59}N$ films was 0.26 [13]. Thirty-two indentations were performed using loads between 6.0 mN and 7.0 mN. The two highest and two lowest values of hardness and elastic modulus measured were not considered for calculating the mean value.

The quality of the adhesion of the films to the substrates of non-nitrated steel and nitrated steel (duplex treatment) was evaluated through the Rockwell C test according to the DIN-CEN/TS 1071-8 standard. In this test, a microhardness tester Brivo VA Reicherter with a maximum load of 1470 N and an optical microscope Olympus CX31, Infinity 1 TH4-100, were used. Three indentations were performed in each deposition condition. An optical microscope developed the images of the damage caused to the film's surface with an image magnification of 100:1.

3. RESULTS

3.1. Plasma nitrated surface

3.1.1. Hardness profile

The thickness of the diffusion layer was determined indirectly using the DIN 50.190 standard and the microhardness profile, measured from the surface of the plasma nitrated steel to the core of the sample. According to the indentations, the nitrated steel had a diffusion layer with an approximate thickness of $60 \pm 10 \mu m$ and microhardness in the core of approximately $712 \pm 6 HV$.

Depending on the amount of N_2 gas used during the plasma nitriding process, a layer of compounds (γ' - Fe_4N and ϵ - $Fe_{2-3}N$) can be formed [14, 15]. Among the mentioned phases, the diffusion coefficient of nitrogen in the compound γ' - Fe_4N ($8.1 \times 10^{-14} m^2/s$) is approximately two orders of magnitude smaller than the diffusion coefficient of α -iron ($6.5 \times 10^{-12} m^2/s$), which favors the formation of the γ' - Fe_4N phase and a thinner diffusion zone [16]. To increase the ion bombardment and obtain a thicker diffusion layer, N_2 or Ar is inserted into the reactor. Ar ions (higher atomic mass) provide energy to the lattice and promote the greater diffusion of nitrogen atoms. With greater diffusion of nitrogen atoms, the layer of compounds tends not to be formed and the diffusion zone increases in thickness [17].

Figure 2 illustrates the microhardness profile performed on nitrated steel.

3.1.2. Crystalline structures

Figure 3 shows the X-ray diffraction spectra of plasma nitrated AISI D2 tool steel.

Chromium nitride (CrN) (ICSD-192945) with face-centered cubic structure (space group 225) was observed in the 2θ positions at 37.5° , 43.5° , and 63.2° ; the Cr_2N phase (ICSD-67400) with trigonal structure

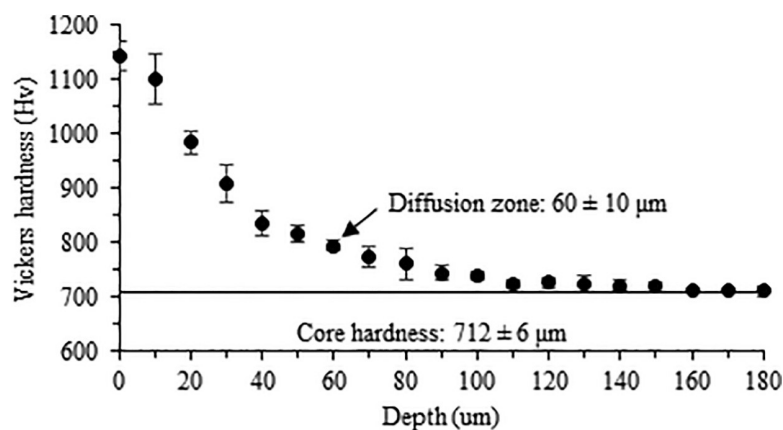


Figure 2: Vickers microhardness profile of AISI D2 tool steel nitrated with 5% N_2 by volume for 120.0 ± 0.5 minutes.

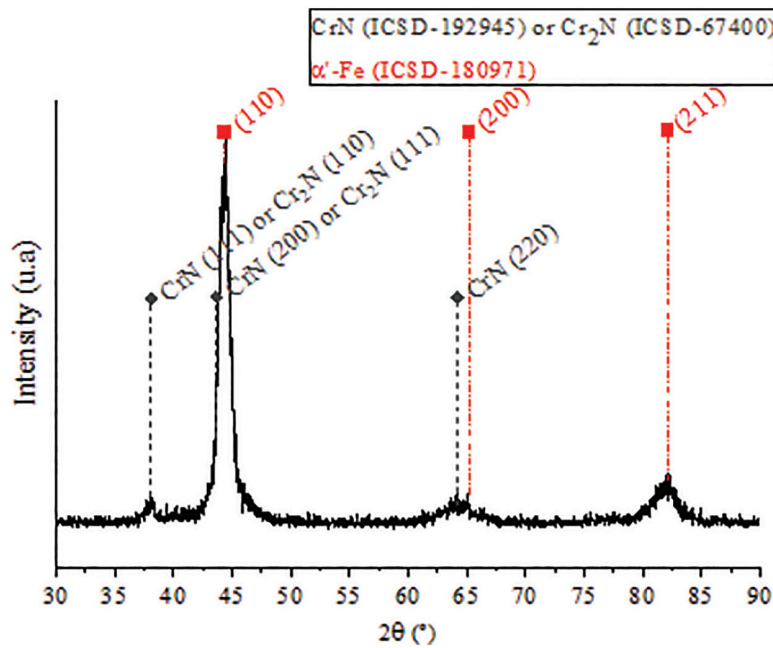


Figure 3: X-ray diffraction pattern (XRD) of the nitrided steel surface.

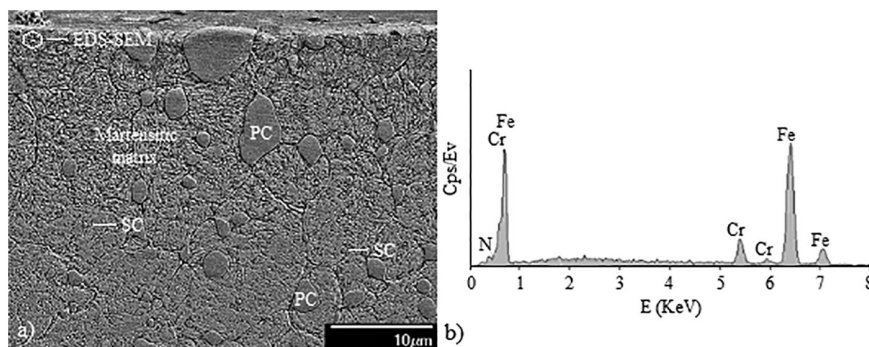


Figure 4: (a) Microstructure of the nitrided steel layer. Cross-section, with 1.0% nital etching for 10 ± 1 seconds, obtained by SEM, (b) Elemental mapping of plasma nitrided steel using EDS-SEM.

(space group 162) in the 2θ positions at 37.5° and 43.5° ; and tetragonal nitrogen-martensite phase (α' -Fe(N)) [1, 18] in the 2θ positions at 44.4° , 64.9° , and 82.2° , with preferential plan development (110).

The primary carbides present in AISI D2 tool steel are rich in Cr. During the plasma nitriding process, nitrogen diffuses into the martensitic matrix and carbides close to the surface, which favors the formation of chromium nitride, in this case, CrN (ICSD-192945) with a face-centered cubic structure (space group 225) and Cr₂N (ICSD-67400) with trigonal structure (space group 162). The presence of primary carbides in plasma nitrided steel was revealed by cross-section via SEM and is illustrated in Figure 4.

The X-ray diffraction spectra of nitrided steel did not detect the formation of diffraction lines of the crystalline phases constituting the layer of compounds (γ' -Fe₄N and ϵ -Fe₂₋₃N).

In this work, the flow of N₂ gas and the process parameters were determined to inhibit the formation of the layer of compounds. The absence of the white layer can induce compressive residual stresses on the nitrided surface. The diffusion zone, absent of γ' -Fe₄N and ϵ -Fe₂₋₃N nitrides, increases the substrate's ability to withstand loading, thus improving the film-substrate adhesion [19].

3.1.3. Microstructures

Figures 4-a and 4-b show the elemental mapping of plasma nitrided steel using EDS-SEM.

The cross-sectional image shows the martensitic matrix, primary carbides (PC), and secondary carbides (SC). Retained austenite and the composite layer (white layer) were not observed.

The EDS-SEM spectrum revealed that the analyzed region contains nitrogen, chromium, and iron. The primary carbides are rich in chromium and the martensitic matrix in α' -iron. Secondary carbides are formed by chromium and nitrogen. EDS-SEM analysis conforms to the XRD spectrum shown in Figure 3.

3.2. TiN and $Ti_{0.41}Al_{0.59}N$ films

3.2.1. Crystalline structures

Figure 5 shows the X-ray diffraction pattern of TiN films deposited on plasma nitrided AISI D2 steel (duplex treatment).

Through the X-ray diffractogram, two diffracted lines approach the α -Ti crystalline phase with a compact hexagonal structure in the 2θ positions at 35.2° and 38.5° with preferential plane development (002). The α -Ti phase corresponds to the intermediate layer deposited between the coating and the substrate.

The diffraction lines of the martensitic matrix were identified in the X-ray diffraction spectra in the 2θ positions at 44.8° with preferential plane development (110), 65.1° , and 82.6° .

The X-ray diffraction spectra also confirmed the presence of the TiN phase (ICSD-152807) with a face-centered cubic structure (space group 225). Figure 5 and Table 4 show that diffraction lines approaching the TiN phase were identified in six different 2θ positions with the development of the preferential plane (111).

Figure 6 shows the X-ray diffraction pattern of $Ti_{0.41}Al_{0.59}N$ films deposited on plasma nitrided AISI D2 steel (duplex treatment).

The X-ray diffraction spectra in Figure 6 show that diffracted lines approaching the $Ti_{0.41}Al_{0.59}N$ phase (ICSD-58012) with face-centered cubic structure (space group 225) were identified in the 2θ positions at 37.7° , 43.3° , 63.6° , and 74.9° with the development of a preferential plan (200).

3.2.2. Microstructures

Figures 7-a and 7-b show that columnar microstructures were formed in both films, similar to the microstructure of the T zone proposed by Thornton [20]. The fibrous grains do not have well-defined boundaries. This characteristic may be related to the deposition conditions used during the nucleation and growth of the films. The formation of the Ti phase between the TiN coating and the silicon substrate is still observed. The middle layer of Ti is 80 ± 5 nm thick.

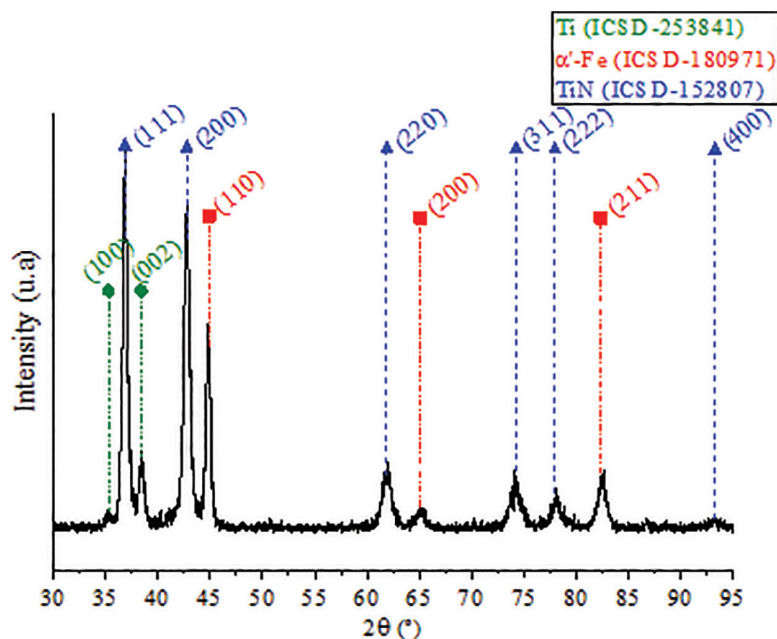


Figure 5: X-ray diffraction pattern of TiN films deposited on plasma nitrided steel.

Table 4: Reference values of the TiN crystalline phase shown in the X-ray diffractograms of Figure 5.

| NUMBER | CRYSTALLINE PLANE | 2 θ (°) | D _{hkl} (nm) | EXPERIMENTAL a (nm) | THEORETICAL a (nm) |
|--------|-------------------|----------------|-----------------------|---------------------|--------------------|
| 1 | (111) | 36.9 ± 0.1 | 2.44 ± 0.05 | 4.22 ± 0.01 | 4.24 |
| 2 | (200) | 42.8 ± 0.1 | 2.11 ± 0.05 | 4.22 ± 0.01 | 4.24 |
| 3 | (220) | 61.9 ± 0.1 | 1.50 ± 0.05 | 4.24 ± 0.01 | 4.24 |
| 4 | (311) | 74.1 ± 0.1 | 1.28 ± 0.05 | 4.24 ± 0.01 | 4.24 |
| 5 | (222) | 78.1 ± 0.1 | 1.23 ± 0.05 | 4.24 ± 0.01 | 4.24 |
| 6 | (400) | 93.2 ± 0.1 | 1.06 ± 0.05 | 4.24 ± 0.01 | 4.24 |

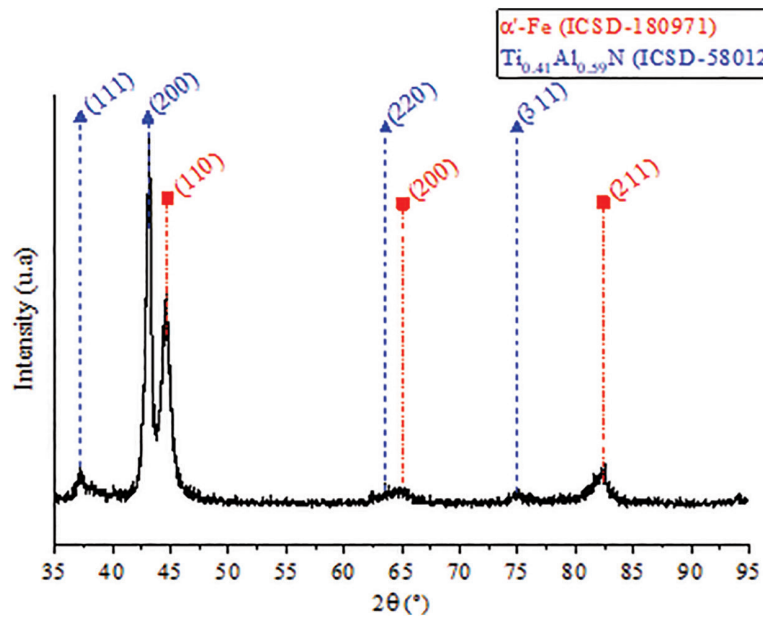


Figure 6: X-ray diffraction pattern of $Ti_{0.41}Al_{0.59}N$ films deposited on nitrated steel.

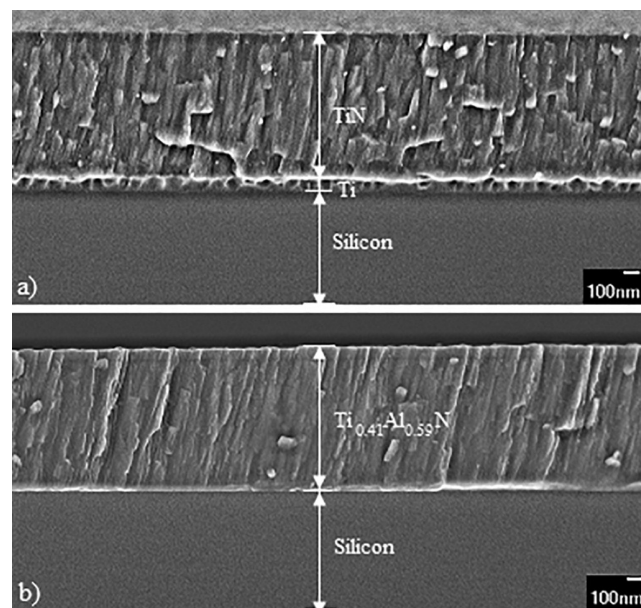


Figure 7: Microstructure images of films via SEM. (a) TiN and (b) TiAlN.

Table 5 shows the average film thickness and deposition rate values.

The TiN and $Ti_{0.41}Al_{0.59}N$ films were obtained with a thickness of $0.8 \pm 0.1 \mu m$ and $0.9 \pm 0.1 \mu m$, respectively. The deposition rate was determined through the ratio between the average thickness of the films and the total deposition time. The deposition rate in both films was $15 \pm 1 \text{ nm/min}$.

3.2.3. Hardness and elastic modulus

Table 6 shows the average values for the hardness and the young modulus of the films deposited on the plasma nitrided AISI D2 tool steel and non-nitrided steel.

There were no significant variations in the hardness and elastic modulus values between the coatings obtained by reactive sputtering deposition and duplex treatment. However, large values can be observed for the mean standard deviation in the elastic modulus of TiN and $Ti_{0.41}Al_{0.59}N$ films deposited on plasma nitrided AISI D2 tool steel and non-nitrided steel. This is explained by the low load (between 6.0 mN and 7.0 mN) applied in the instrumented indentation test and the surface roughness.

Table 5: Average thickness of films deposited on silicon.

| FILM | AVERAGE FILM THICKNESS (μm) | DEPOSITION TIME (min) | DEPOSITION RATE (nm/min) |
|-----------------------|------------------------------------|-----------------------|--------------------------|
| TiN | 0.8 ± 0.1 | 54.0 ± 0.5 | 15 ± 1 |
| $Ti_{0.41}Al_{0.59}N$ | 0.9 ± 0.1 | 60.0 ± 0.5 | 15 ± 1 |

Table 6: Hardness (H) and elastic modulus (E) of TiN and TiAlN thin films via IIT.

| COATING | TREATMENT | HARDNESS (GPa) | YOUNG MODULUS (GPa) |
|---------|--|----------------|---------------------|
| TiN | Duplex: plasma nitriding and reactive deposition | 25 ± 1 | 331 ± 25 |
| TiN | Reactive deposition | 24 ± 2 | 296 ± 21 |
| TiAlN | Duplex: plasma nitriding and reactive deposition | 23 ± 2 | 320 ± 30 |
| TiAlN | Reactive deposition | 21 ± 4 | 317 ± 28 |

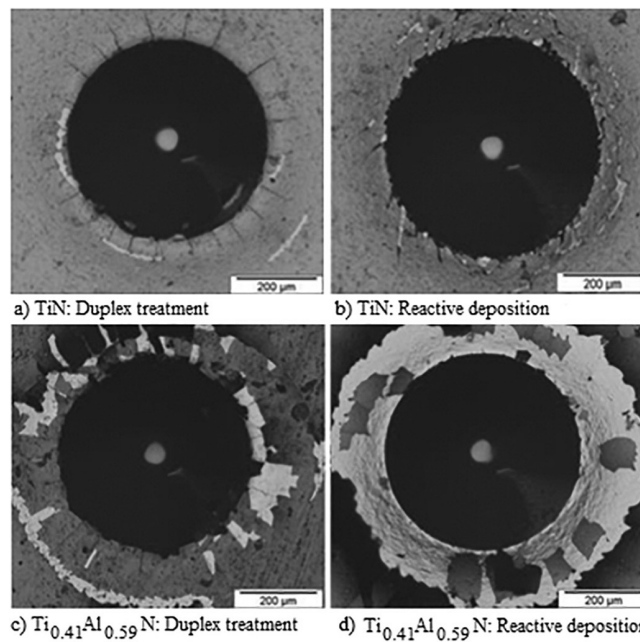


Figure 8: Rockwell C test of film adhesion to the substrate. (a) TiN obtained via duplex treatment, (b) TiN obtained via reactive deposition, (c) $Ti_{0.41}Al_{0.59}N$ obtained via duplex treatment, and (d) $Ti_{0.41}Al_{0.59}N$ obtained via reactive deposition.

3.2.4. Film-substrate adhesion

The adhesion of TiN and $Ti_{0.41}Al_{0.59}N$ films to plasma nitrided AISI D2 tool steel and non-nitrided steel was qualitatively evaluated – DIN Standard – CEN/TS 1071-8.

Figures 8-a and 8-b show the damage caused to the indented surfaces of TiN films deposited on plasma nitrided steel (duplex treatment) and non-nitrided steel, respectively. The images show the presence of microcracks and some circular cracks. These films have acceptable adhesion and are rated HF-1 and HF-2, respectively.

$Ti_{0.41}Al_{0.59}N$ coatings with a N_2 flow rate of 6.8 ± 0.2 sccm deposited by duplex treatment have moderate spalling and few microcracks (Figure 8-c). The samples are characterized with the HF-4 index. Coatings deposited on non-nitrided steel produced a large peeling area, characteristic of the HF-6 adhesion index (Figure 8-d).

It is observed that the films obtained by the duplex treatment, compared to those deposited on non-nitrided steel, presented the best indices of quality of adhesion of the coatings to the substrates. The compressive loads acting on the nitrided layer may have influenced the adhesion of the films to the substrates. Compressive loads provide mechanical support to the substrate surface thus promoting an increase in load loading and unloading capacity [9, 21, 22].

The improvement in the quality of adhesion of the coating to the plasma nitrided substrate discussed in this work conforms to the research by Recco *et al.* [5] and Dalke *et al.* [22]. Recco *et al.* [5] evaluated the adhesion quality of TiN on H13 steel substrates. They concluded that the improvement in the coating-substrate adhesion occurred due to the pre-treatment of the substrate via plasma nitriding. Likewise, Dalke *et al.* [22] obtained Cr-Al-Ti-B-N films via duplex treatment. The authors concluded that the surface hardening of the substrate via nitriding influenced improving the coating-substrate adhesion quality.

4. CONCLUSIONS

In both films obtained, the formation of the face-centered cubic phase (space group 225) can be observed. TiN films showed preferential plane development (111), and $Ti_{0.41}Al_{0.59}N$ films showed preferential plane development (200).

The coatings obtained by duplex treatment exhibited hardness and elastic modulus highest values using the same deposition conditions as those deposited on non-nitrided steel.

The films obtained via duplex treatment were evaluated as having the best indices of quality of adhesion of the film to the substrate when compared with the films deposited on non-nitrided steel. TiN samples deposited on plasma nitrided steel and non-nitrided steel with a N_2 flow rate of 4.6 ± 0.1 sccm were characterized as HF-1 and HF-2 index (acceptable adhesion), respectively. $Ti_{0.41}Al_{0.59}N$ coatings deposited with a N_2 flow rate of 6.8 ± 0.2 sccm on plasma nitrided steel were characterized by HF-4 index (acceptable adhesion). However, the films deposited on the non-nitrided steel exhibited a large exposed surface area of the substrate, thus characterized by the HF-6 index (non-acceptable adhesion).

5. ACKNOWLEDGEMENT

To the Department of Physics and the Department of Mechanical Engineering of the Graduate Program in Materials Science and Engineering at the State University of Santa Catarina – UDESC, at Joinville, Brazil.

6. BIBLIOGRAPHY

- [1] DÍAZ-GUILLÉN, J.C., NAEEM, M., HDZ-GARCÍA, H.M., “Duplex plasma treatment of AISI D2 tool steel by combining plasma nitriding (with and without white layer) and post-oxidation”, *Surface and Coatings Technology*, v. 385, pp. 1–14, Jan. 2020. doi: <http://dx.doi.org/10.1016/j.surfcoat.2020.125420>.
- [2] OKONKWO, P.C., KELLY, G., ROLFE, B.F., *et al.*, “The effect of temperature on sliding wear of steel-tool steel pairs”, *Wear*, v. 283, pp. 22–30, Jan. 2012. doi: <http://dx.doi.org/10.1016/j.wear.2012.01.017>.
- [3] DAS, A.K., SHARIFF, S.M., CHOUDHURY, A.R., “Effect of rare earth oxide (Y2O3) addition on alloyed layer synthesized on Ti-6Al-4V substrate with Ti+SiC+h-BN mixed precursor by laser surface engineering”, *Tribology International*, v. 95, pp. 35–43, Nov. 2015. doi: <http://dx.doi.org/10.1016/j.triboint.2015.10.035>.
- [4] HÖRLING, A., HULTMAN, L., ODÉN, M., *et al.*, “Mechanical properties and machining performance of Ti1- xAlxN-coated cutting tools”, *Surface and Coatings Technology*, v. 191, n. 2–3, pp. 384–392, Jun. 2004. doi: <http://dx.doi.org/10.1016/j.surfcoat.2004.04.056>.
- [5] RECCO, A.A.C., OLIVEIRA, I.C., MASSI, M., *et al.*, “Adhesion of reactive magnetron sputtered TiNx and TiCy coatings to AISI H13 tool steel”, *Surface and Coatings Technology*, v. 202, n. 4–7, pp. 1078–1083, Aug. 2007. doi: <http://dx.doi.org/10.1016/j.surfcoat.2007.07.073>.

- [6] KOVACI, H., HACISALIHOĞLU, İ., YETIM, A.F., *et al.*, “Effects of shot peening pre-treatment and plasma nitriding parameters on the structural, mechanical and tribological properties of AISI 4140 low-alloy steel”, *Surface and Coatings Technology*, v. 358, pp. 256–265, Jan. 2019. doi: <http://dx.doi.org/10.1016/j.surfcoat.2018.11.043>.
- [7] ROUSSEAU, A.F., PARTRIDGE, J.G., MAYES, E.L.H., *et al.*, “Microstructural and tribological characterization of a nitriding/TiAlN PVD coating duplex treatment applied to M2 High Speed Steel tools”, *Surface and Coatings Technology*, v. 272, pp. 403–408, Apr. 2015. doi: <http://dx.doi.org/10.1016/j.surfcoat.2015.03.034>.
- [8] ABREU, L.H.P., PIMENTEL, M.C.L., BORGES, W.F.A., *et al.*, “Plasma nitriding of AISI M2 steel: Performance evaluation in forming tools”, *Surface Engineering*, v. 36, n. 5, Jan, pp. 508–515, 2020. doi: <http://dx.doi.org/10.1080/02670844.2020.1727685>.
- [9] TORRES, R.D., SOARES JUNIOR, P.C., SCHMITZ, C., *et al.*, “Influence of the nitriding and TiAlN/TiN coating thickness on the sliding wear behavior of duplex treated AISI H13 steel”, *Surface and Coatings Technology*, v. 205, n. 5, pp. 1381–1385, Aug. 2010. doi: <http://dx.doi.org/10.1016/j.surfcoat.2010.07.102>.
- [10] RECCO, A.A.C., “*Estudo da obtenção e das propriedades dos filmes de TiN e TiC depositados sobre aços ferramentas AISI H13 e D2 nitretados e não nitretados*”, Tese de D.Sc., Universidade de São Paulo, São Paulo, 2008. doi: <http://dx.doi.org/10.11606/T.3.2008.tde-16042009-140247>.
- [11] FONTANA, L.C., MUZART, J.L.R., “Triode magnetron sputtering TiN film deposition”, *Surface and Coatings Technology*, v. 114, n. 1, pp. 7–12, Jan. 1999. doi: [http://dx.doi.org/10.1016/S0257-8972\(99\)00032-8](http://dx.doi.org/10.1016/S0257-8972(99)00032-8).
- [12] BUNSHAH, R.F., *Handbook of hard coating: deposition technologies, properties and application*, New York, William Andrew, 2001.
- [13] HE, Y., SCHWARZ, B.R., MIGLIORI, A.E., *et al.*, “Elastic constants of single crystal γ -TiAl”, *Materials Research Society*, v. 10, n. 5, pp. 1187–1195, May. 1995. doi: <http://dx.doi.org/10.1557/JMR.1995.1187>.
- [14] DAS, K., ALPHONSA, J., GHOSH, M., *et al.*, “Influence of pretreatment on surface behavior of duplex plasma treated AISI H13 tool steel”, *Surfaces and Interfaces*, v. 8, pp. 206–213, Jun. 2017. doi: <http://dx.doi.org/10.1016/j.surfin.2017.06.009>.
- [15] KOVACI, H., YETIM, A., BARAN, Ö., *et al.*, “Fatigue crack growth analysis of plasma nitrided AISI 4140 low-alloy steel”, *Materials Science and Engineering*, v. 672, pp. 257–275, Aug. 2016. doi: <http://dx.doi.org/10.1016/j.msea.2016.07.002>.
- [16] DIMITROV, V.I., D’HAAN, J., KNUYT, G., *et al.*, “A diffusion model of metal surface modification during plasma nitriding”, *Materials Science & Processing*, v. 63, n. 5, pp. 475–480, Jun. 1996. doi: <http://dx.doi.org/10.1007/BF01571677>.
- [17] CONCI, M.D., BOZZI, A.C., FRANCO JUNIOR, A.R., “Effect of plasma nitriding potential on tribological behaviour of AISI D2 cold-worked tool steel”, *Wear*, v. 317, n. 1-2, pp. 188–193, Jun. 2014. doi: <http://dx.doi.org/10.1016/j.wear.2014.05.012>.
- [18] JACOBSEN, S.D., HINRICHS, R., BAUMVOL, I.J.R., *et al.*, “Depth distribution of martensite in plasma nitrided AISI H13 steel and its correlation to hardness”, *Surface & Coatings Technology*, v. 270, pp. 266–271, May 2015. doi: <http://dx.doi.org/10.1016/j.surfcoat.2015.02.046>.
- [19] SUN, Y., BLOYCE, A., BELL, T., “Finite element analysis of plastic deformation of various TiN coating/substrate systems under normal contact with rigid sphere”, *Thin Solid Films*, v. 271, n. 1-2, pp. 122–131, Jul. 1995. doi: [http://dx.doi.org/10.1016/0040-6090\(95\)06942-9](http://dx.doi.org/10.1016/0040-6090(95)06942-9).
- [20] THORNTON, J.A., “Influence of apparatus geometry and deposition conditions on the structure and topography of thick sputtered coatings”, *Journal of Vacuum Science and Technology*, v. 11, n. 4, pp. 666–670, Jul. 1974. doi: <http://dx.doi.org/10.1116/1.1312732>.
- [21] ALKAN, S., GÖK, M.S., “Influence of plasma nitriding pre-treatment on the corrosion and tribocorrosion behaviours of PVD CrN, TiN and AlTiN coated AISI 4140 steel in seawater”, *Lubrication Science*, v. 34, n. 2, pp. 67–83, Nov. 2021. doi: <http://dx.doi.org/10.1002/lc.1572>.
- [22] DALKE, A., WEINHOLD, T., SCHRAMM, A., *et al.*, “Microstructure and adhesion characteristics of duplex coatings with different plasma-nitrided layers and a Cr-Al-Ti-B-N physical vapor deposition coating”, *Engineering Reports*, v. 4, n. 7-8, pp. 1–14, Feb. 2021. doi: <http://dx.doi.org/10.1002/eng2.12364>.